Geochemistry, Geophysics, Geosystems

RESEARCH ARTICLE
10.1029/2019GC008621

Key Points:
- Earth's oxygen cycle and marine acid-base balance are linked
- Long-term transfer of oxidizing power between crustal reservoirs helps buffer marine pH
- Net redox shifts within Earth's crust can drive significant changes to marine pH, carbon cycling, and climate state

Supporting Information:
- Supporting Information S1

Correspondence to:
C. T. Reinhard,
chris.reinhard@eas.gatech.edu

Citation:
Reinhard, C. T., & Fischer, W. W. (2019). Mechanistic Links Between the Sedimentary Redox Cycle and Marine Acid-Base Chemistry. *Geochemistry, Geophysics, Geosystems*, *20*, 5968–5978. https://doi.org/10.1029/2019GC008621

Received 27 AUG 2019
Accepted 18 NOV 2019
Accepted article online 26 NOV 2019
Published online 10 DEC 2019

Mechanistic Links Between the Sedimentary Redox Cycle and Marine Acid-Base Chemistry

Christopher T. Reinhard[1,2] and Woodward W. Fischer[3]

[1]School of Earth and Atmospheric Sciences, Georgia Institute of Technology, Atlanta, GA, USA, [2]NASA Astrobiology Institute, Mountain View, CA, USA, [3]Division of Geological and Planetary Sciences, California Institute of Technology, Pasadena, CA, USA

Abstract The redox state of Earth's surface is controlled on geological timescales by the flow of electrons through the sedimentary rock cycle, mediated largely by the weathering and burial of C-S-Fe phases. These processes buffer atmospheric pO_2. At the same time, CO_2 influxes and carbonate burial control seawater acid-base chemistry and climate over long timescales via the carbonate-silicate cycle. However, these two systems are mechanistically linked and impact each other via charge balance in the hydrosphere. Here, we use a low-order Earth system model to interrogate a subset of these connections, with a focus on changes that occur during perturbations to electron flow through the sedimentary rock cycle. We show that the net oxidation or reduction of the Earth's surface can play an important role in controlling acid-base processes in the oceans and thus climate, and suggest that these links should be more fully integrated into interpretive frameworks aimed at understanding Earth system evolution throughout Precambrian and Phanerozoic time.

1. Introduction

The stability of Earth's long-term carbon cycle and climate system are conventionally viewed to be maintained by the crustal "Urey cycle," which involves the exchange of carbon between the solid and fluid Earth reservoirs through volcanism, metamorphism, chemical alteration of Earth's crust, and the burial of authigenic carbon-bearing phases in marine sediments (Ebelmen, 1845; Urey, 1952). In particular, the response of silicate mineral weathering in the upper crust to both surface temperature and runoff (e.g., Caldeira & Kasting, 1992; Krissanson-Totton & Catling, 2017; Ridgwell & Zeebe, 2005; Tajika & Matsui, 1992; Walker et al., 1981; Zeebe & Caldeira, 2008) provides a negative feedback that regulates Earth's long-term atmospheric CO_2 level as a function of volcanic and metamorphic outgassing from the solid Earth. This planetary titration of volatile acids by weathering of the Earth's crust—followed by removal of carbonate and other salts in marine sediments—plays a crucial role in regulating Earth's atmosphere, climate, and seawater chemistry on geological timescales (Archer et al., 1997; Berner et al., 1983).

In a similar fashion, the oxygen (O_2) abundance in Earth's atmosphere and the overall redox state of the ocean-atmosphere system are largely controlled by the flow of electrons through the crust and between the exogenic system (crust-ocean-atmosphere) and Earth's interior (Berner & Canfield, 1989; Garrels & Perry, 1974; Hayes & Waldbauer, 2006; Holland, 2009; Kump & Garrels, 1986). The consumption rates of O_2 by alteration of continental and oceanic crust are also dependent on ocean-atmosphere O_2 levels (Bach & Edwards, 2003; Chang & Berner, 1999; Williamson & Rimstidt, 1994), though in ways that are not well understood quantitatively. Nevertheless, the transfer of C, S, and Fe between oxidized and reduced reservoirs in the crust and marine sediments plays a crucial role in controlling Earth's atmospheric O_2 level and the redox state of the ocean-atmosphere system.

Though implicit in many previous studies of Earth's coupled C-S-O_2-Fe cycles (e.g., Lasaga et al., 1985), there has been a recently burgeoning interest in the modes of coupling between the classical carbonate-silicate-CO_2 system and the sedimentary redox cycle—the set of processes controlling the net transfer of electrons between C, S, and Fe species in the crust-ocean-atmosphere system (Bachan & Kump, 2015; Higgins et al., 2009; Tziperman et al., 2011). These recent discussions have primarily focused on the role of electron transfer within the oceans rather than on net electron flow within the crust and between the crust and ocean, and there has been limited (though profitable) exploration of the potentially important links between the rock

cycle of crustal sulfide minerals and nonsteady-state atmospheric CO_2 levels (e.g., Calmels et al., 2007; Torres et al., 2014). Earlier large-scale biogeochemical models implicitly link planetary redox and the carbonate-silicate system but either impose steady-state mass balance in all cycles simultaneously (e.g., Berner, 2006) or do not explicitly solve for the chemistry of the marine carbonate system (Bergman et al., 2004). Here, we attempt to provide a step toward more explicitly bridging these approaches via implementation of a low-order Earth system model designed specifically to test and explore the corollary processes that regulate redox balance and acid-base equilibrium in the ocean-atmosphere-crust system.

2. Conceptual Framework

The oxidative weathering of crustal sulfide minerals results in the production of proton (H^+) equivalents:

$$2FeS_2 + 7.5O_2 + 4H_2O \rightarrow Fe_2O_3 + 4SO_4^{2-} + 8H^+ \quad (1)$$

These H^+ equivalents can be buffered by dissolution of carbonate rocks and/or silicate minerals, or they can accumulate in solution and drive the pH of surface waters to lower values—in effect representing a net flux of H^+ equivalents from the crust to the ocean-atmosphere system. In the case of buffering by crustal carbonate phases, the process liberates inorganic carbon and calcium from the crust and generates a flux of alkalinity:

$$CaCO_3 + H^+ \rightarrow Ca^{2+} + HCO_3^- \quad (2)$$

Ultimately, the calcium, inorganic carbon, and alkalinity released by this process are balanced by the consumption of dissolved inorganic carbon and alkalinity during the formation and burial of carbonate mineral phases in marine sediments (e.g., Berner et al., 1983):

$$Ca^{2+} + 2HCO_3^- \rightarrow CaCO_3 + CO_2 + H_2O \quad (3)$$

Because each mole of CO_2 released during $CaCO_3$ formation and burial is not initially derived from the atmosphere (as is the case during crustal carbonate weathering driven by carbonic acid formation in rainwater), this represents a net source of CO_2 to the ocean-atmosphere system. However, this CO_2 can be balanced, along with the SO_4^{2-} released during the initial sulfide oxidation step above, by photosynthetic carbon fixation in the surface ocean (equation (4)) coupled with microbial sulfate reduction (equation (5)) and the formation and burial of pyrite sulfur in marine sediments (equation (6)):

$$CO_2 + H_2O \rightarrow CH_2O + O_2 \quad (4)$$

$$2CH_2O + SO_4^{2-} \rightarrow H_2S + 2HCO_3^- \quad (5)$$

$$8H_2S + 2Fe_2O_3 + O_2 \rightarrow 4FeS_2 + 8H_2O \quad (6)$$

Examining the stoichiometry of the above reactions, it becomes clear that on arbitrarily long timescales these coupled processes will have no net effect on the ocean-atmosphere carbon balance. However, because the CO_2 released by the process is buffered by the seawater SO_4^{2-} reservoir these processes can lead to transient net fluxes of CO_2 to the ocean-atmosphere system (Calmels et al., 2007; Ross et al., 2018) that can persist on geological timescales and may in turn have long-term impacts on global climate (Torres et al., 2014).

Alternatively, the H^+ equivalents generated by equation (1) can be buffered by the dissolution of crustal silicates (for simplicity shown here as wollastonite):

$$CaSiO_3 + 2H^+ \rightarrow Ca^{2+} + H_4SiO_4 \quad (7)$$

The calcium liberated by this process will ultimately be balanced by formation and burial of $CaCO_3$ in marine sediments. As above, this process releases CO_2 that is balanced together with the SO_4^{2-} released in equation (1) by photosynthetic carbon fixation and the operation of the crustal pyrite subcycle. In contrast to the

situation that arises via crustal carbonate weathering, these coupled processes actually represent an overall sink for ocean-atmosphere carbon on arbitrarily long timescales via the net reaction:

$$CaSiO_3 + 2CO_2 + H_2O \rightarrow CaCO_3 + H_4SiO_4 \quad (8)$$

Canonically, the siliceous acid produced in this process does not impact long-term acid-base balance because it is ultimately converted to SiO_2 [but see Isson & Planavsky, 2018]. In any case, these coupled processes result in a net transfer of ocean-atmosphere carbon to the solid reservoir of $CaCO_3$ in recycling sediments.

In what follows, we construct a simple biogeochemical model meant to take into account the downstream impacts of channeling proton equivalents through either carbonate or silicate weathering, and to link together the carbonate-silicate cycle with the global oxygen cycle. For illustrative purposes our model represents the fluxes of carbon, alkalinity, calcium, sulfate, and oxygen according to the conceptual framework discussed above. However, we emphasize that this is an end-member formulation—much of the crustal silicate mass cycling at Earth's surface can differ in its mineralogy from the simple scenario depicted above, and at present it remains difficult to fully represent the complexity of crustal Fe-bearing mineral reservoirs (e.g., carbonate, silicate, oxide, and sulfide phases) in a universal fashion. Nevertheless, we consider such a framework a useful step forward in better understanding the mechanistic links between changes in Earth surface redox and marine carbonate chemistry.

3. A Simple Model of Proton Mass Balance

Our approach takes a similar tack to previous models developed to explore the basic dynamics of coupled C-S-O_2 cycling (Bergman et al., 2004; Berner et al., 1983; Kump & Garrels, 1986). Briefly, the model considers the Earth's ocean-atmosphere system as a single, well-mixed reservoir at gas exchange equilibrium and solves mass balance expressions for total ocean-atmosphere carbon, seawater alkalinity, marine calcium and sulfate, and atmospheric oxygen. Our model, therefore, does not diagnose variations in the ocean's alkalinity balance that occur more rapidly than that of typical mixing timescales for ocean basins. Solid Earth fluxes (e.g., volcanic and mid-ocean ridge CO_2 input) are imposed, while the weathering of silicate-carbonate-sulfide minerals and organic carbon in the crust are parameterized as functions of either surface temperature and runoff or atmospheric pO_2 (Bergman et al., 2004; Berner et al., 1983; Kump & Garrels, 1986; Maher & Chamberlain, 2014; West, 2012). Surface temperature is specified by a simple climate system, in which a base temperature—governed by the assumption of a single-layer gray atmosphere at radiative equilibrium—is modified by a radiative forcing that depends on atmospheric greenhouse gas content (Chamberlain, 1980; Lenton, 2000; Mills et al., 2011). We follow Mills et al. (2011) in including both a primary kinetic weathering term and a maximum weathering rate, meant to represent the notion that silicate/carbonate weathering can be "transport limited" at very high rates of weathering (e.g., Hilley et al., 2010; West et al., 2005). Carbonate burial in marine sediments and seafloor silicate weathering both depend on the marine carbonate system and are parameterized following Tziperman et al. (2011) and Le Hir et al. (2008), respectively. Organic carbon and pyrite sulfur burial in marine sediments are also parameterized to respond to ocean-atmosphere O_2 levels (see supporting information).

A schematic of the principal processes in our model is given in Figure 1, while a full description of the model structure and mass balance expressions is provided in the supporting information. In addition to more highly parameterized responses of weathering/burial of reduced carbon and sulfur to ocean-atmosphere O_2 levels, we elaborate on previous treatments (Berner & Beerling, 2007; Kump & Arthur, 1999; Torres et al., 2014) by explicitly specifying a more inclusive series of linkages between the Earth surface sulfur cycle and the acid-base balance of the ocean-atmosphere system. This is accomplished primarily via terms in the mass balance expressions that represent the relative partitioning of the H^+ equivalents generated through the oxidation of crustal sulfide minerals through either crustal carbonate dissolution, crustal silicate weathering, or an "unbuffered" flux of H^+ equivalents according to the reaction stoichiometries outlined above. This allows us to assess in greater detail the role of imbalances in the sedimentary redox cycle in regulating the marine carbonate system and atmospheric chemistry.

In what follows, we examine the results of perturbations to the model in which the weathering of reduced C and S phases in the Earth's crust and marine sediments is rapidly increased and then allowed to evolve

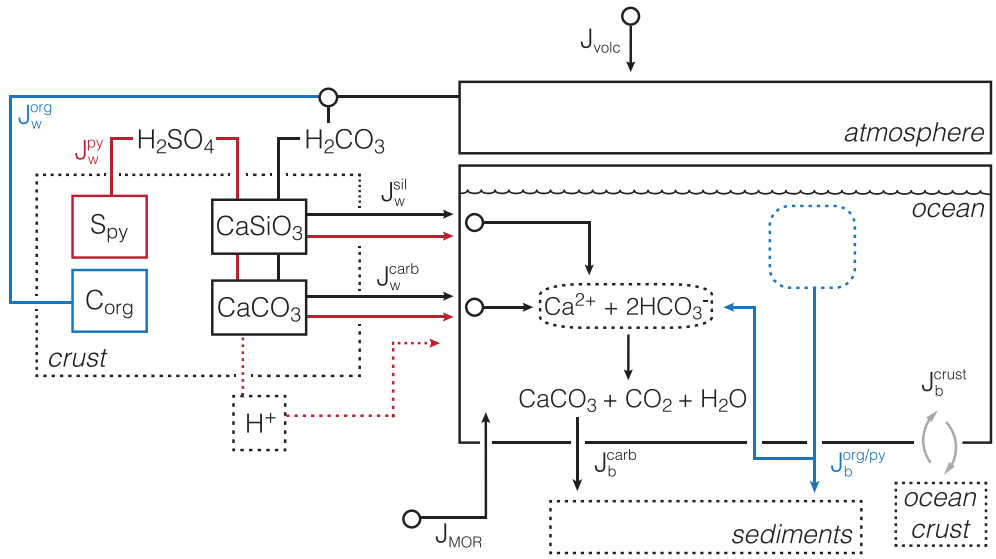

Figure 1. Schematic of the Earth system model discussed in the text, highlighting the key interactions between redox and acid-base processes. The ocean-atmosphere system is taken as a single reservoir with respect to carbon and oxygen and interacts with the crust and marine sediments through weathering and burial of oxidized and reduced carbon/sulfur species. The model explicitly tracks oceanic reservoirs of dissolved organic carbon (DIC), alkalinity (Alk), calcium (Ca^{2+}), sulfate (SO_4^{2-}), atmospheric O_2 and CO_2, and crust/sediment reservoirs of pyrite/evaporite sulfur and organic/carbonate carbon. *J* terms are fluxes with the subscripts denoting weathering (w) and burial (b), and the superscripts reflecting organic (org), silicate (sil), carbonate (carb), pyrite (pyr). See Tables S1–S4 for detailed model equations and parameter values.

dynamically. We then explore the dynamics of shorter, transient perturbations to crustal weathering rates. Finally, we evaluate the potential effects of electron flow through the Earth's crust/sediment system on adjustment to changes in the rates of solid Earth degassing. These perturbations can be considered physically as secular or transient shifts in global erosion rate, the weatherability of exposed crust/sediments sourcing reduced carbon and sulfur, and long-term changes in rates of volcanism and outgassing. We stress that our aim here is to generally explore the links between the flow of redox and acid-base equivalents through the crust-ocean-atmosphere system rather than precisely quantify the effects of any particular perturbation scenario, and our focus is on the potential impacts of redox imbalance within the rock cycle in controlling acid-base chemistry rather than the construction of a more comprehensive model of seawater charge balance (e.g., Halevy & Bachan, 2017). However, in describing the general model results we briefly discuss some of these mechanics in the context of Neoproterozoic "Snowball Earth" glaciations—known intervals of acid-base perturbation (Higgins & Schrag, 2003; Hoffman et al., 1998) that could owe some of their behavior to changes in redox processes also observed at that time.

4. Model Analyses: Basic Response and Sensitivity

All simulations are initialized as hypothetical "late Proterozoic" steady states (see supporting information), which differ somewhat in their stable carbon and alkalinity fluxes depending on the mode in which proton equivalents are channeled through the crust associated with oxidative weathering. However, the accuracy of these states is secondary to our purposes here. Spinup to steady state conditions is described in the supporting information. A given steady state is then tracked in a time-dependent fashion through a series of perturbations in which dimensionless weathering area factors (f_i^A) are initially increased and the weathering responses are then allowed to evolve dynamically in accordance with the feedback parameterizations described in the supporting information. The following perturbations are explored here: (1) an initial doubling of pyrite sulfur weathering (increase in $f_{py}{}^A$ by a factor of 2), (2) an initial doubling of both pyrite sulfur and organic carbon weathering (increase in both $f_{py}{}^A$ and $f_{org}{}^A$ by a factor of 2), and (3) an initial 50% increase in all crustal weathering rates (increase in $f_{py}{}^A$, $f_{org}{}^A$, $f_{sil}{}^A$, and $f_{ev}{}^A$ by a factor of 0.5). The first two of these are loosely motivated by several key observations from the sedimentary record of

Neoproterozoic glacial intervals: the accumulation and diagenetic stabilization of synglacial iron formation lithologies with unusually large detrital contributions and a dominantly ferric (hematite) mineralogy (Klein, 2005) with little evidence of organic diagenesis—observations standing in stark contrast to Archean and Paleoproterotoic iron formation (Fischer & Knoll, 2009), and large ^{17}O mass anomalies (Bao et al., 2008) that require an atypical lack of sulfur cycling in Earth surface environments to be preserved. Both of these sets of observations imply major changes in the redox balance between oxidative weathering and reduced C/S burial in favor of net O_2 consumption. The last is meant to represent a generalized period of elevated overall surface erosion/weathering rates, as is likely to have occurred many times throughout Earth's geologic history. Indeed, petrogenic organic carbon oxidation appears to be enhanced in some rapidly eroding regions of Earth's surface (Horan et al., 2017), suggesting that in some regions weathering rates of all the dominant crustal phases considered in our model will rise and fall in parallel.

All perturbations are imposed as a logistic function, with an adjustment timescale of 500 kyr. These perturbation modes are designed to gradually isolate the effects of the reduced carbon/sulfur subcycles (2) and the pyrite sulfur subcycle (1) from the conventional carbonate/silicate cycle (3). Mechanistically, they could represent sustained uplift and chemical erosion of a mafic igneous terrane or large ore deposit (1), the exhumation and weathering of a large package of sedimentary rocks (2; deposited, e.g., in a long-lived epieric seaway), or a major change in overall continental denudation (3). More broadly, it is possible to imagine large intervals of Earth's history (or on other ocean-bearing silicate planets that have contrasting differentiation histories) during which net electron transfer between crustal phases are largely decoupled due to changes in the principal crustal reservoirs hosting each phase (Hurowitz et al., 2010; Kamber, 2010). Although the approximate magnitudes of these shifts are in keeping with long-term and transient changes inferred for Earth's history (Ozaki et al., 2019; Them et al., 2017; Wilkinson & McElroy, 2007), our aim is to assess the basic behavior of the model to changes in electron flow through the crust and marine sediments rather than simulate any particular event in the rock record or any specific mechanistic scenario. Perturbations and adjustments to weathering rates are shown in Figure 2.

Shown in Figure 2 are atmospheric partial pressures of CO_2 (pCO_2)—a useful diagnostic for model changes in surface temperature and carbonate burial. When proton equivalents are channeled toward the dissolution of crustal carbonate minerals, secular increases in pyrite S weathering yield significant increases in atmospheric pCO_2. This release is largely balanced on long timescales despite permanently elevated pyrite weathering rates (Figures 2a–2c), consistent with the analysis of (Torres et al., 2014), and the conceptual framework discussed above (Calmels et al., 2007). Notably, the adjustment timescale, maximum pCO_2, and relative steady-state pCO_2 values before and after the secular shift in pyrite weathering rates are strongly modulated by the reservoir size of SO_4^{2-} in seawater and by coupled increases in the exhumation and weathering of other crustal phases (e.g., organic C and silicate minerals). For instance, for an isolated increase in pyrite S weathering, varying baseline SO_4^{2-} concentrations between 0.2 and 20 mM results in large relative differences in peak pCO_2 and the timescale of transient CO_2 release (Figure 2d). In these simulations the dependence of the overall response on SO_4^{2-} concentration is muted significantly by coupled increases in pyrite S and organic C weathering (Figure 2e), highlighting the importance of the globally integrated weathering ratio of reduced C and S in controlling atmospheric composition. Finally, when all crustal weathering rates are increased in parallel, the timescales of net CO_2 release is strongly contingent on the reservoir size of seawater SO_4^{2-} (Figure 2f).

Experiments in which proton equivalents are instead channeled toward the dissolution of crustal silicate minerals show somewhat different behavior (Figures 2g–2i). First, sulfide-catalyzed silicate weathering is a net CO_2 sink on arbitrarily long timescales, consistent with the common view of silicate weathering outlined above (Figure 2g). Though this CO_2 removal can be counteracted by parallel increases in organic C oxidation (Figure 2h), peak CO_2 is strongly attenuated relative to the case of crustal carbonate buffering (Figure 2e) and significant long-term CO_2 drawdown still occurs despite the coupled secular change in reduced C/S weathering. In all cases (both "carbonate-buffered" and "silicate-buffered") the shifts in atmospheric pCO_2 are sufficiently large to strongly impact Earth's climate system.

Next, we explore the dynamics of the model during transient perturbations to the weathering of reduced carbon and sulfur in the crust, such as might occur during a Phanerozoic isotopic excursion. In this case, $f_{py}{}^{A}$ for sulfide weathering is initially doubled and weathering rates are allowed to adjust dynamically for 2 million

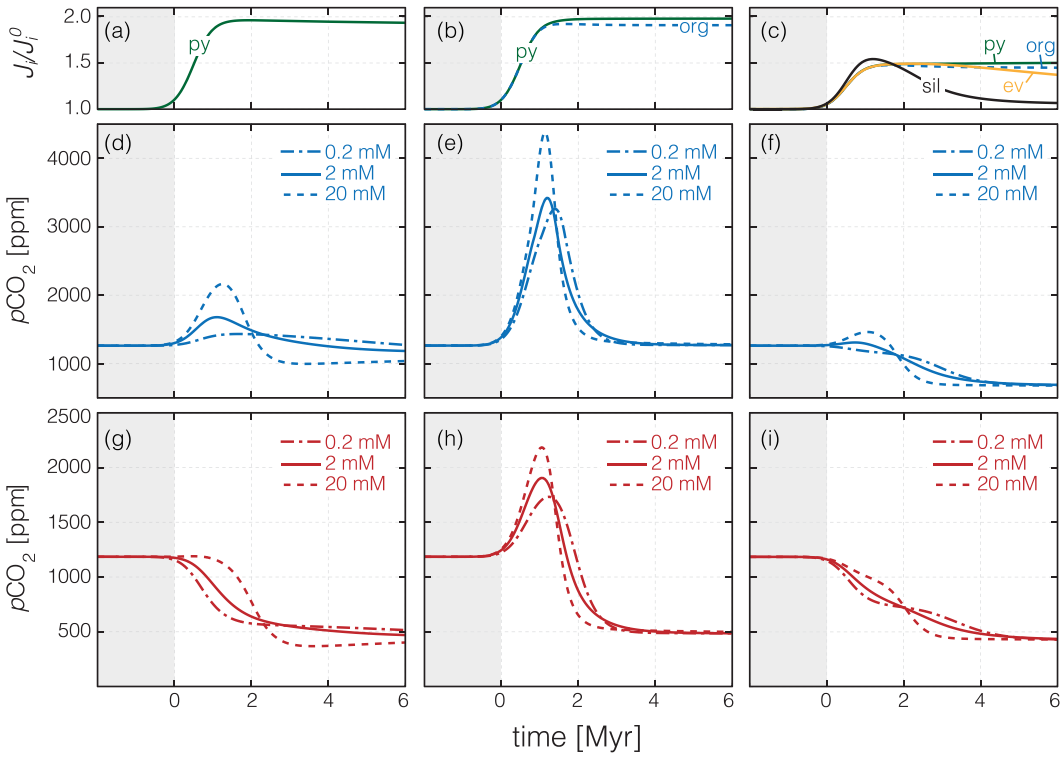

Figure 2. Atmospheric pCO_2 changes during secular perturbation to crustal weathering rates. A secular initial increase was applied to pyrite sulfur oxidation (doubling), coupled pyrite sulfur and organic carbon oxidation (doubling), and parallel weathering of all crustal phases represented in the model (50% increase). Panels (a)–(c) show the relative crustal weathering fluxes for pyrite (py), organic carbon (org), crustal silicates (sil), and sulfate evaporites (ev). In (d)–(f), proton equivalents produced during crustal sulfide oxidation are channeled through carbonate dissolution, while in (g)–(i) they are channeled through crustal silicate dissolution. Curves are labeled according to initial seawater SO_4^{2-} concentration (in mM), with dash-dot, solid, and dashed curves denoting initial seawater SO_4^{2-} concentrations of 200 μM, 2 mM, and 20 mM, respectively.

years, after which $f_{py}{}^A$ is brought back to the original value (Figure 3). Trajectories in pO_2-pH space capture the dynamic links between atmospheric oxygenation and seawater acid-base balance in the model, with the scale of variation controlled by seawater [SO_4^{2-}]. In addition, it is clear that transient imbalances in weathering and burial of reduced C and S in the crust and marine sediments can lead to significant shifts in alkalinity fluxes and marine carbonate overproduction or underproduction (e.g., transient storage of alkalinity in the oceans; Figures 3c and 3d). These are generally of a slightly greater magnitude for simulations in which proton equivalents from sulfide oxidation are channeled through crustal carbonate dissolution and also adjust more rapidly than scenarios in which these proton equivalents are buffered by silicate minerals in the crust (Figures 3c and 3d). Importantly, these effects would be potentially observable via both proxies for seawater carbonate chemistry (e.g., $\delta^{11}B$) and sequence stratigraphic variations in carbonate accumulation rates (e.g., Sadler, 1994; Zachos et al., 2005), particularly when marine SO_4^{2-} is elevated. For instance, in the case of the Neoproterozoic Snowball Earth cap carbonates, our results suggest that some of the acid-base perturbation marked by boron isotope trends (Kasemann et al., 2005) and the syncopated underproduction and overproduction of carbonate lithotypes (Hoffman et al., 1998) could have been aided by synglacial increases in relative amounts of oxidative weathering versus reduced C and S burial.

Lastly, we explore the behavior of our model when subjected to secular perturbations in solid Earth degassing. A series of reference simulations is run in which volcanic CO_2 fluxes are increased by 50% according to a logistic function with an adjustment time of 100 kyr and are maintained at elevated values for millions of years—for example, the emplacement of a large igneous province or increased rates of subduction and/or interaction of magmatic arc systems with carbonates along the margin of an ocean basin (Kerrick &

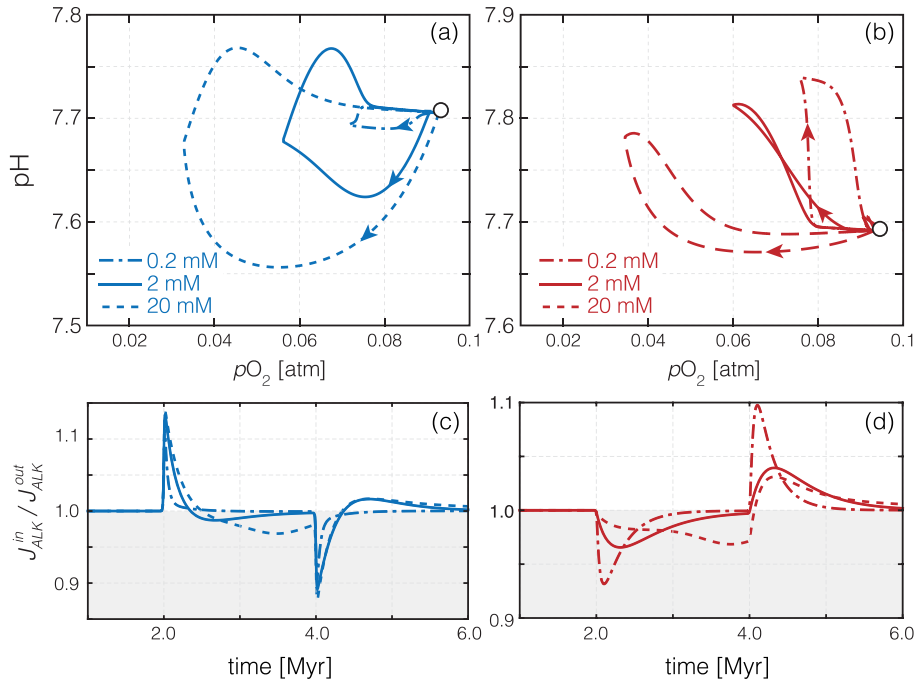

Figure 3. Phase portraits showing atmospheric pO_2 and ocean pH (a, b) and seawater alkalinity flux balance (c, d) for transient perturbations to crustal weathering rates. Results are shown for simulations in which crustal sulfide weathering was transiently doubled according to a step function with an adjustment timescale of 1 million years. In (a) and (b), the sense of time in these hystereses is clockwise in all cases (denoted by arrows). In (c) and (d), curves show the ratio between alkalinity input and output fluxes, showing periods of overproduction and underproduction of carbonate (with overproduction denoted by the shaded area). In (a) and (c), proton equivalents produced during crustal sulfide oxidation are channeled through carbonate dissolution, while in (b) and (d) they are channeled through crustal silicate dissolution. Dash-dot, solid, and dashed curves denote initial seawater SO_4^{2-} concentrations of 200 μM, 2 mM, and 20 mM, respectively.

Caldeira, 1998; Lee et al., 2013). A second series of simulations is then run in which this increase in volcanic CO_2 input is accompanied by an increase in volcanic reductant input to 4 Tmol year^{-1} (O_2 equivalents). In absolute flux terms, this is roughly equivalent to a doubling of the modern solid Earth volatile reductant flux of ~2 Tmol year^{-1} O_2 equivalents (Kasting & Canfield, 2012). It is important to note that we are not explicitly releasing any particular suite of volcanic gases in the model—we simply add an input flux of reducing equivalents to diagnose the effects of dynamic ocean-atmosphere redox on the overall system response to increased CO_2 degassing. The two sets of simulations are then differenced, and relative anomalies (e.g., Δ values) calculated based on the "combined flux" simulations minus the reference simulations. Results of these simulations are shown in Figure 4.

It is clear that redox fluxes can have a significant impact on the Earth system response to increases in volcanism, irrespective of the mode of proton equivalent buffering during crustal sulfide oxidation. In the model results there is modulation by the reservoir size of SO_4^{2-} in seawater, but this appears to be a secondary effect. This reflects the overriding influence of the crust/sediment organic carbon subcycle in regulating both Earth surface redox and the climate system. For example, as volcanic reductant input increases, atmospheric pO_2 adjusts downward, and results in a decrease in CO_2 release during petrogenic organic carbon weathering and a net transfer of carbon from the atmosphere to the sedimentary organic pool (e.g., Figures 4b and 4e). The overall effect can have a nontrivial impact on CO_2 and climate (Figures 4c and 4f). However, the "CO_2-only" simulations are not entirely decoupled from the redox system: the mobilization of Ca^{2+} from the crust can influence marine $CaSO_4$ burial, with downstream impacts on [SO_4^{2-}], sedimentary pyrite burial, and ocean-atmosphere O_2 levels. Thus, the results of these simulations may underestimate the potential relative importance of "redox" and "nonredox" processes in adjusting to changes in solid Earth degassing.

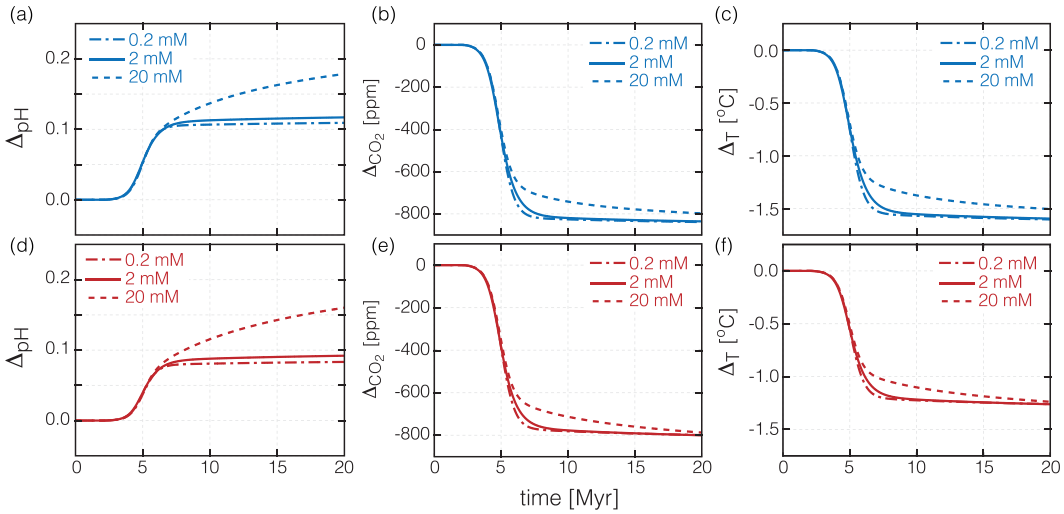

Figure 4. Relative changes in seawater pH (Δ_{pH}; a, d), atmospheric pCO_2 (Δ_{CO2}; b, e), and Earth surface temperature (Δ_T; c, f) during secular perturbations to rates of volcanism. Rates of volcanism are increased at 2 Myr according to a logistic function with an adjustment time of 100kyr, after which the model evolves freely. Values for "Δ" represent the difference between a simulation in which volcanic CO_2 inputs are increased by 50% and volcanic fluxes are increased to 4 Tmol year^{-1} of O_2 equivalents and reference simulations in which only volcanic CO_2 fluxes are increased. Note that overall, atmospheric pCO_2 will still rise despite a negative value for $_{CO2}$. Blue curves (a–c) represent simulations in which proton equivalents from sulfide oxidation are channeled through crustal carbonate dissolution, while red curves (d–f) represent simulations in which proton equivalents are channeled through weathering of crustal silicates. Dash-dot, solid, and dashed curves denote initial seawater SO_4^{2-} concentrations of 200 μM, 2 mM, and 20 mM, respectively.

5. Discussion and Extensions

Transient and secular increases in the weathering of rocks rich in reduced C and S and long-term changes in rates of solid Earth degassing should be expected to lead to coupled changes in atmosphere and ocean redox budgets, dissolved inorganic carbon and alkalinity throughput, and seawater acid-base balance. Importantly, our results illustrate that these flux adjustments are strongly controlled by redox imbalances in the organic C subcycle and that the ultimate effects can be strongly amplified or counteracted by imbalances in the pyrite S subcycle depending on the ultimate fate of the proton equivalent flux generated during pyrite weathering and the size of the marine SO_4^{2-} inventory. As a result of these couplings, the effect strength and adjustment time during perturbations to redox balance in the sedimentary rock cycle is controlled in large part by the major ion chemistry of seawater (e.g., SO_4^{2-} concentration and Ca^{2+}/SO_4^{2-} ratio) and the factors that govern the mode of proton equivalent buffering within the pyrite S subcycle—for example, lithotypes exposed for weathering at the Earth surface, meridional distribution of exposed carbonate and/or silicate (e.g., arc) rock packages, and long-term patterns in the secular chemical evolution of the Earth's upper crust (e.g., Dhuime et al., 2012; Keller & Schoene, 2012). In particular, the globally integrated weathering ratio of reduced C and S in the crust is important for regulating atmospheric chemistry and carbonate system adjustment.

The overall effects of solid Earth degassing at Earth's surface are also linked to the crust/sediment redox system. For instance, the impact of widespread and protracted arc volcanism should depend strongly on the chemistry of the crust being processed within the arc system, and subsequent atmospheric adjustment will depend on the dynamics of crustal weathering during arc exhumation (Lee et al., 2015). The implication is that not all long-term perturbations to solid Earth degassing are created equal, and the net effect of such perturbations will be shaped by the global balance of arc and hot-spot volcanism, its links to hydrothermal gases and fluids as controlled by seawater chemistry (Kump & Seyfried, 2005), and in the case of arc systems both the type of arc "substrate" and the latitude and local climate prevailing along the arc. For example, increased subduction of pelagic carbonate (e.g., Caldeira, 1992; Volk, 1989) at a relatively constant global heat flow will potentially have significantly different effects than an overall increase in heat flow through the crust, particularly if this increase is offset to some degree by seawater-basalt interaction (e.g., a change in reductant fluxes from the solid Earth, and oxidative weathering of igneous phases).

We expect that the basic responses of the model behavior to these types of perturbations are robust. However, a full understanding of these relationships with respect to effect strength and accuracy of the characteristic timescales will ultimately require more explicit representations of the chemical heterogeneity and spatial distribution of Earth's regolith, spatial variation in marine carbonate burial, more mechanistic coupling to heat flow and solid Earth degassing, and the targeted application of empirical tests of acid-base fluctuations predicted by inferred redox shifts (and vice-versa). In addition, there are potentially more intimate and detailed links between Earth surface redox and the processing of Earth's weathering surface than explored here, such as the potential control of overall chemical erosion by O_2 supply to depth in weathering profiles (e.g., Brantley & Lebedeva, 2011). In turn, these relationships should depend strongly on the substrate and flow conditions in a given weathering environment—features that can be difficult to capture in low-order Earth system models.

Nevertheless, we stress that these linkages make testable predictions that should be evident in elemental, isotopic, and sequence stratigraphic sedimentary records. Changes in the long-term cycling of carbon and sulfur through the ocean-atmosphere-crust system should be accompanied by observable changes in the acid-base balance of the oceans, while many changes in the marine carbonate system should leave evidence in the record of Earth surface redox. For example, long-term flux imbalances invoked to explain large C- or S-isotope perturbations during Precambrian and Phanerozoic time could potentially be further constrained by empirical data aimed at assessing relative carbonate production rates. These relationships also predict that exceptional perturbations to the ocean's carbonate system, such as the late Proterozoic "Snowball Earth" events (Higgins & Schrag, 2003), either are a direct outgrowth of or were accompanied by notable perturbations to Earth surface redox and atmospheric pO_2.

Acknowledgments
C. T. R. acknowledges funding support from the National Science Foundation, NASA Astrobiology Institute, and Alfred P. Sloan Foundation. W. W. F. acknowledges funding support from the Agouron Institute and David & Lucille Packard Foundation. C. T. R. acknowledges support from the O.K. Earl Fellowship at the California Institute of Technology. Data Availability All model code and scripts for postprocessing and plotting are hosted on GitHub. The specific version of the code used in this paper is tagged as release v1.0 and can be obtained by cloning (https://github.com/reinhard-lab/carb.chem.git) or downloading (https://github.com/reinhard-lab/carb.chem/releases/) and is assigned a DOI:10.5281/zenodo.3560099.

References

Archer, D., Kheshgi, H., & Maier-Reimer, E. (1997). Multiple timescales for neutralization of fossil fuel CO_2. *Geophysical Research Letters*, *24*, 405–408.

Bach, W., & Edwards, K. J. (2003). Iron and sulfide oxidation within the basaltic ocean crust: Implications for chemolithoautotrophic microbial biomass production. *Geochimica et Cosmochimica Acta*, *67*, 3871–3887.

Bachan, A., & Kump, L. R. (2015). The rise of oxygen and siderite oxidation during the Lomagundi Event. *Proceedings of the National Academy of Sciences, USA*, *112*, 6562–6567.

Bao, H., Lyons, J. R., & Zhou, C. (2008). Triple oxygen isotope evidence for elevated CO_2 levels after a Neoproterozoic glaciation. *Nature*, *453*(7194), 504–506. https://doi.org/10.1038/nature06959

Bergman, N. M., Lenton, T. M., & Watson, A. J. (2004). COPSE: A new model of biogeochemical cycling over Phanerozoic time. *American Journal of Science*, *304*, 397–437.

Berner, R. A. (2006). GEOCARBSULF: A combined model for Phanerozoic atmospheric O2 and CO_2. *Geochimica et Cosmochimica Acta*, *70*, 5653–5664.

Berner, R. A., & Beerling, D. J. (2007). Volcanic degassing necessary to produce a CaCO3 undersaturated ocean at the Triassic-Jurassic boundary. *Palaeogeography, Palaeoclimatology, Palaeoecology*, *244*, 368–373.

Berner, R. A., & Canfield, D. E. (1989). A new model for atmospheric oxygen over Phanerozoic time. *American Journal of Science*, *289*, 333–361.

Berner, R. A., Lasaga, A. C., & Garrels, R. M. (1983). The carbonate-silicate geochemical cycle and its effect on atmospheric carbon dioxide over the past 100 million years. *American Journal of Science*, *283*, 641–683.

Brantley, S. L., & Lebedeva, M. (2011). Learning to read the chemistry of regolith to understand the Critical Zone. *Annual Review of Earth and Planetary Sciences*, *39*, 387–416.

Caldeira, K. (1992). Enhanced Cenozoic chemical weathering and the subduction of pelagic carbonate. *Nature*, *357*, 578–581.

Caldeira, K., & Kasting, J. F. (1992). The life span of the biosphere revisited. *Nature*, *360*(6406), 721–723. https://doi.org/10.1038/360721a0

Calmels, D., Gaillardet, J., Brenot, A., & France-Lanord, C. (2007). Sustained sulfide oxidation by physical erosion processes in the Mackenzie River basin: Climatic perspectives. *Geology*, *35*, 1003–1006.

Chamberlain, J. W. (1980). Changes in the planetary heat balance with chemical changes in air. *Planetary and Space Science*, *28*, 1011–1018.

Chang, S., & Berner, R. A. (1999). Coal weathering and the geochemical carbon cycle. *Geochimica et Cosmochimica Acta*, *63*, 3301–3310.

Dhuime, B., Hawkesworth, C. J., Cawood, P. A., & Storey, C. D. (2012). A change in the geodynamics of continental growth 3 billion years ago. *Science*, *335*(6074), 1334–1336. https://doi.org/10.1126/science.1216066

Ebelmen, J. J. (1845). Sur les produits de la décomposition des especes minérales de la famille des silicates. *Ann. des Mines*, *7*, 3–66.

Fischer, W. W., & Knoll, A. H. (2009). An iron shuttle for deep-water silica in Late Archean and Early Paleoproterozoic iron formation. *Geological Society of America Bulletin*, *121*, 222–235.

Garrels, R. M., & Perry, E. A. (1974). *Cycling of carbon, sulfur, and oxygen through geologic time. The Sea* (Vol. 5, pp. 303–336). New York: Wiley Interscience.

Halevy, I., & Bachan, A. (2017). The geologic history of seawater pH. *Science*, *355*(6329), 1069–1071. https://doi.org/10.1126/science.aal4151

Hayes, J. M., & Waldbauer, J. R. (2006). The carbon cycle and associated redox processes through time. *Phil. Trans. R. Soc. B*, *361*, 931–950.

Higgins, J. A., Fischer, W. W., & Schrag, D. P. (2009). Oxygenation of the ocean and sediments: Consequences for the seafloor carbonate factory. *Earth and Planetary Science Letters*, *284*, 25–33.

Higgins, J. A., & Schrag, D. P. (2003). Aftermath of a snowball Earth. *Geochemistry, Geophysics, Geosystems*, *4*(3). https://doi.org/10.1029/2002GC000403

Hilley, G. E., Chamberlain, C. P., Moon, S., Porder, S., & Willett, S. D. (2010). Competition between erosion and reaction kinetics in controlling silicate-weathering rates. *Earth and Planetary Science Letters*, *293*, 191–199.

Hoffman, P. F., Kaufman, A. J., Halverson, G. P., & Schrag, D. P. (1998). A Neoproterozoic Snowball Earth. *Science*, *281*(5381), 1342–1346. https://doi.org/10.1126/science.281.5381.1342

Holland, H. D. (2009). Why the atmosphere became oxygenated: A proposal. *Geochimica et Cosmochimica Acta*, *73*, 5241–5255.

Horan, K., Hilton, R. G., Selby, D., Ottley, C. J., Gröcke, D. R., Hicks, M., & Burton, K. W. (2017). Mountain glaciation drives rapid oxidation of rock-bound organic carbon. *Science Advances*, *3*, e1701107.

Hurowitz, J. A., Fischer, W. W., Tosca, N. J., & Milliken, R. E. (2010). Origin of acidic surface waters and the evolution of atmospheric chemistry on early Mars. *Nature Geoscience*, *3*, 323–326.

Isson, T. T., & Planavsky, N. J. (2018). Reverse weathering as a regulator of marine pH, climate stability, and cooling. *Nature*, *560*(7719), 471–475. https://doi.org/10.1038/s41586-018-0408-4

Kamber, B. S. (2010). Archean mafic-ultramafic volcanic landmasses and their effect on ocean-atmosphere chemistry. *Chemical Geology*, *274*, 19–28.

Kasemann, S. A., Hawkesworth, C. J., Prave, A. R., Fallick, A. E., & Pearson, P. N. (2005). Boron and calcium isotope composition in Neoproterozoic carbonate rocks from Namibia: Evidence for extreme environmental change. *Earth and Planetary Science Letters*, *231*, 73–86.

Kasting, J. F., & Canfield, D. E. (2012). In A. H. Knoll, D. E. Canfield, & K. O. Konhauser (Eds.), *The global oxygen cycle. Fundamentals of Geobiology* (Vol. 456). Hoboken, NJ: Blackwell Publishing Ltd.

Keller, C. B., & Schoene, B. (2012). Statistical geochemistry reveals disruption in secular lithospheric evolution about 2.5 Gyr ago. *Nature*, *485*, 490–493.

Kerrick, D. M., & Caldeira, K. (1998). Metamorphic CO_2 degassing from orogenic belts. *Chemical Geology*, *145*, 213–232.

Klein, C. (2005). Some Precambrian banded iron-formations (BIFs) from around the world: Their age, geologic setting, mineralogy, metamorphism, geochemistry, and origin. *American Mineralogist*, *90*, 1473–1499.

Krissanson-Totton, J., & Catling, D. C. (2017). Constraining climate sensitivity and continental versus seafloor weathering using an inverse geological carbon cycle model. *Nature Communications*, *8*.

Kump, L. R., & Arthur, M. A. (1999). Interpreting carbon-isotope excursions: Carbonates and organic matter. *Chem. Geol.*, *161*, 181–198.

Kump, L. R., & Garrels, R. M. (1986). Modeling atmospheric O_2 in the global sedimentary redox cycle. *Am. J. Sci.*, *286*, 337–360.

Kump, L. R., & Seyfried, W. E. Jr. (2005). Hydrothermal Fe fluxes during the Precambian: Effect of low oceanic sulfate concentrations and low hydrostatic pressure on the composition of black smokers. *Earth and Planetary Science Letters*, *235*, 654–662.

Lasaga, A. C., Berner, R. A., & Garrels, R. M. (1985). An improved geochemical model of atmospheric CO_2 fluctuations over the past 100 million years. *Geophysical Monograph Series*, *32*, 397–411.

Le Hir, G., Goddéris, Y., Donnadieu, Y., & Ramstein, G. (2008). A geochemical modelling study of the evolution of the chemical composition of seawater linked to a "snowball" glaciation. *Biogeosciences*, *5*, 253–267.

Lee, C. A., Shen, B., Slotnick, B. S., Liao, K., Dickens, G. R., Yokoyama, Y., et al. (2013). Continental arc-island arc fluctuations, growth of crustal carbonates, and long-term climate change. *Geosphere*, *9*, 21–36.

Lee, C. T. A., Thurner, S., Paterson, S., & Cao, W. (2015). The rise and fall of continental arcs: Interplays between magmatism, uplift, weathering, and climate. *Earth and Planetary Science Letters*, *425*, 105–119.

Lenton, T. M. (2000). Land and ocean carbon cycle feedback effects on global warming in a simple Earth system model. *Tellus*, *52B*, 1159–1188.

Maher, K., & Chamberlain, C. P. (2014). Hydrologic regulation of chemical weathering and the geologic carbon cycle. *Science*, *343*(6178), 1502–1504. https://doi.org/10.1126/science.1250770

Mills, B., Watson, A. J., Goldblatt, C., Boyle, R., & Lenton, T. M. (2011). Timing of Neoproterozoic glaciations linked to transport-limited global weathering. *Nature Geoscience*, *4*, 861–864.

Ozaki, K., Reinhard, C. T., & Tajika, E. (2019). A sluggish mid-Proterozoic biosphere and its effect on Earth's redox balance. *Geobiology*, *17*(1), 3–11. https://doi.org/10.1111/gbi.12317

Ridgwell, A., & Zeebe, R. E. (2005). The role of the global carbonate cycle in the regulation and evolution of the Earth system. *Earth and Planetary Science Letters*, *234*, 299–315.

Ross, M. R. V., Nippgen, F., Hassett, B. A., McGlynn, B. L., & Bernhardt, E. S. (2018). Pyrite oxidation drives exceptionally high weathering rates and geologic CO_2 release in mountaintop-mined landscapes. *Global Biogeochemical Cycles*, *32*, 1182–1194.

Sadler, P. M. (1994). The expected duration of upward-shallowing peritidal carbonate cycles and their terminal hiatuses. *Geological Society of America Bulletin*, *106*, 791–802.

Tajika, E., & Matsui, T. (1992). Evolution of terrestrial proto-CO_2 atmosphere coupled with thermal history of the earth. *Earth and Planetary Science Letters*, *113*, 251–266.

Them, T. R., Gill, B. C., Selby, D., Gröcke, D. R., Friedman, R. M., & Owens, J. D. (2017). Evidence for rapid weathering response to climatic warming during the Toarcian Oceanic Anoxic Event. *Nature Scientific Reports*, *7*, 5003.

Torres, M. A., West, A. J., & Li, G. (2014). Sulphide oxidation and carbonate dissolution as a source of CO_2 over geological timescales. *Nature*, *507*(7492), 346–349. https://doi.org/10.1038/nature13030

Tziperman, E., Halevy, I., Johnston, D. T., Knoll, A. H., & Schrag, D. P. (2011). Biologically induced initiation of Neoproterozoic snowball-Earth events. *Proceedings of the National Academy of Sciences, USA*, *108*, 15,091–15,096.

Urey, H. C. (1952). *The planets: Their origin and development*. New Haven: CT, Yale University Press.

Volk, T. (1989). Sensitivity of climate and atmospheric CO_2 to deep-ocean and shallow-ocean carbonate burial. *Nature*, *337*, 637–640.

Walker, J. C. G., Hays, P. B., & Kasting, J. F. (1981). A negative feedback mechanism for the long-term stabilization of Earth's surface temperature. *Journal of Geophysical Research*, *86*, 9776–9782.

West, A. J. (2012). Thickness of the chemical weathering zone and implications for erosional and climatic drivers of weathering and for carbon-cycle feedbacks. *Geology*, *40*, 811–814.

West, A. J., Galy, A., & Bickle, M. (2005). Tectonic and climatic controls on silicate weathering. *Earth and Planetary Science Letters*, *235*, 211–228.

Wilkinson, B. H., & McElroy, B. J. (2007). The impact of humans on continental erosion and sedimentation. *GSA Bulletin*, *119*, 140–156.

Williamson, M. A., & Rimstidt, J. D. (1994). The kinetics and electrochemical rate-determining step of aqueous pyrite oxidation. *Geochimica et Cosmochimica Acta*, *58*, 5443–5454.

Zachos, J. C., Röhl, U., Schellenberg, S. A., Sluijs, A., Hodell, D. A., Kelly, D. C., et al. (2005). Rapid acidification of the ocean during the Paleocene-Eocene Thermal Maximum. *Science*, *308*, 1611–1615.

Zeebe, R. E., & Caldeira, K. (2008). Close mass balance of long-term carbon fluxes from ice-core CO_2 and ocean chemistry records. *Nature Geoscience*, *1*, 312–315.

References From the Supporting Information

Bolton, E. W., Berner, R. A., & Petsch, S. T. (2006). The weathering of sedimentary organic matter as a control on atmospheric O2: II. *Theoretical modeling, American Journal of Science*, *306*, 575–615.

Byrne, B., & Goldblatt, C. (2014). Radiative forcing at high concentrations of well-mixed greenhouse gases. *Geophysical Research Letters*, *41*, 152–160.

Canfield, D. E. (1994). Factors influencing organic carbon preservation in marine sediments. *Chemical Geology*, *114*, 315–329.

Canfield, D. E. (2005). The early history of atmospheric oxygen: Homage to Robert M. Garrels. *Ann. Rev. Earth Planet. Sci.*, *33*, 1–36.

Halevy, I., Peters, S. E., & Fischer, W. W. (2012). Sulfate burial constraints on the Phanerozoic sulfur cycle. *Science*, *337*(6092), 331–334. https://doi.org/10.1126/science.1220224

Hartnett, H. E., Keil, R. G., Hedges, J. I., & Devol, A. H. (1998). Influence of oxygen exposure time on organic carbon preservation in continental margin sediments. *Nature*, *391*, 572–575.

Hedges, J. I., Hu, F. S., Devol, A. H., Hartnett, H. E., Tsamakis, E., & Keil, R. G. (1999). Sedimentary organic matter preservation: A test for selective degradation under oxic conditions. *American Journal of Science*, *299*, 529–555.

Ozaki, K., & Tajika, E. (2013). Biogeochemical effects of atmospheric oxygen concentration, phosphorus weathering, and sea-level stand on oceanic redox chemistry: Implications for greenhouse climates. *Earth and Planetary Science Letters*, *373*, 129–139.

Petsch, S. T., Berner, R. A., & Eglinton, T. I. (2000). A field study of the chemical weathering of ancient sedimentary organic matter. *Organic Geochemistry*, *31*, 475–487.

Petsch, S. T., Edwards, K. J., & Eglinton, T. I. (2005). Microbial transformations of organic matter in black shales and implications for global biogeochemical cycles. *Palaeogeography, Palaeoclimatology, Palaeoecology*, *219*, 157–170.

Reinhard, C. T., Planavsky, N. J., Robbins, L. J., Partin, C. A., Gill, B. C., Lalonde, S. V., et al. (2013). Proterozoic ocean redox and biogeochemical stasis. *Proceedings of the National Academy of Sciences USA*, *110*, 5357–5362.

Wildman, R. A., Berner, R. A., Petsch, S. T., Bolton, E. W., Eckert, J. O., Mok, U., & Evans, J. B. (2004). The weathering of sedimentary organic matter as a control on atmospheric O2: I. *Analysis of a black shale, American Journal of Science*, *304*, 234–249.